2017

Eugenol Nanoencapsulated by Sodium Caseinate: Physical, Antimicrobial, and Biophysical Properties

Yue Zhang
University of Nebraska-Lincoln, yue.zhang@unl.edu

Kang Pan
University of Tennessee

Qixin Zhong
University of Tennessee, qzhong@utk.edu

Published in *Food Biophysics* (2017), doi 10.1007/s11483-017-9509-0

Submitted 6 November 2017; accepted 7 December 2017; published online 14 December 2017.

Eugenol Nanoencapsulated by Sodium Caseinate: Physical, Antimicrobial, and Biophysical Properties

Yue Zhang,[1,2] Kang Pan,[1] and Qixin Zhong[1]

1 Department of Food Science, University of Tennessee, 2510 River Drive, Knoxville, TN 37996, USA
2 Department of Food Science and Technology, University of Nebraska–Lincoln, Lincoln, NE, USA

Corresponding author — Qixin Zhong, qzhong@utk.edu

Abstract
To improve the application of essential oils as natural antimicrobial preservatives, the objective of the present study was to determine physical, antimicrobial, and biophysical properties of eugenol after nanoencapsulation by sodium caseinate (NaCas). Emulsions were prepared by mixing eugenol in 20.0 mg/mL NaCas solution at an overall eugenol content of 5.0–137.9 mg/mL using shear homogenization. Stable emulsions were observed up to 38.5 mg/mL eugenol, which had droplet diameters of smaller than 125 nm at pH 5–9 after ambient storage for up to 30 days. The encapsulated eugenol had similar minimal inhibitory and minimal bactericidal concentrations as free eugenol against *Escherichia coli* O157:H7 ATCC 43895, *Listeria monocytogenes* Scott A, and *Salmonella* Enteritidis but showed better inhibition of *E. coli* O157:H7 than free eugenol during incubation at 37 °C for 48 h. After 20 min interaction at 21 °C, bacteria treated with encapsulated eugenol had a greater reduction of intracellular ATP and a greater increase of extracellular ATP than free eugenol, suggesting the enhanced permeation of eugenol after nanoencapsulation. However, such overall trend was not observed when examining bacterial morphology and uptake of crystal violet, suggesting the possible membrane adaptation. Findings from this study showed the feasibility of preparing nanoemulsions with high loading of eugenol using NaCas.

Keywords: eugenol, sodium caseinate, nanoemulsion, antimicrobial activity, membrane permeability

Introduction

Essential oils (EOs) are secondary metabolites of plants [1]. Many EOs and their components have excellent antimicrobial activities and can potentially be used as natural preservatives to meet the increasing consumer demand

for clean labels [1]. However, poor solubility and high volatility of EOs limit their application in aqueous foods and beverages. This has led to studies of delivery systems to improve their applicability in food matrices. Emulsions [2], food biopolymer particles [3, 4], and liposomes [5] are several groups of colloidal systems studied to encapsulate EOs. In addition to improving the dispersibility of EOs [6, 7], some studies have reported the improved antimicrobial activity of EOs after encapsulation [5]. Conversely, other studies have shown negative effects on antimicrobial activity after encapsulating EOs, which would nullify their practical applications [2, 8, 9]. Therefore, materials used to deliver EOs are to be carefully studied.

For food applications, delivery systems should ideally be fabricated from generally-recognized-as-safe (GRAS) ingredients. To prepare emulsions, dairy proteins are extensively studied as natural emulsifiers due to their abundance, low cost, and amphiphilic properties. Sodium caseinate (NaCas) is a commercially available ingredient that can be used to prepare emulsions due to its excellent surface activity. The self-assembly properties of caseins have been used to nanoencapsulate hydrophobic molecules such as bixin and curcumin [10, 11]. NaCas has been used to encapsulate EO components with and without other ingredients such as zein and lecithin [12–14]. Thymol nanoemulsified by NaCas showed a significant improvement of anti-listerial activity in milk with different fat contents when compared to free thymol [14]. However, much is unknown about the biophysical properties of EO components after nanoencapsulation.

The first objective of this work was to characterize physicochemical and antimicrobial properties of nanoemulsions prepared with eugenol and NaCas. Eugenol was chosen as a model EO component because of extensive research on its antimicrobial activities and the proposed antimicrobial mechanisms [1, 15]. Eugenol is a major component of clove oil and has a higher antibacterial activity than many other phenolic EO compounds or phenol esters such as carvacrol and basil methyl chavicol [1]. Additionally, properties of eugenol after nanoencapsulation by NaCas are unclear. The second objective was to evaluate biophysical changes of bacteria to understand impacts of nanoencapsulation on antimicrobial mechanisms of eugenol against both Gram-negative *Escherichia coli* O157:H7 ATCC 43895 and *Salmonella* Enteritidis, and Gram-positive *Listeria monocytogenes* Scott A.

Materials and Methods

Chemicals

NaCas was a product from American Casein Co. (Burlington, NJ, USA). Eugenol was purchased from Sigma-Aldrich Corp. (St Louis, MO, USA).

High-performance liquid chromatography (HPLC) grade water and methanol (>99% purity) were procured from Fisher Scientific (Pittsburgh, PA, USA). Other chemicals were from either Sigma-Aldrich or Fisher Scientific.

Preparation of Nanoemulsions

NaCas was hydrated at 20.0 mg/mL in deionized water overnight at room temperature (RT, 21 °C), and the dispersion pH was measured to be 6.8. Different amounts of eugenol were mixed with the NaCas solution. The mixtures were then homogenized at 8000 rpm for 3 min using a Cyclone I.Q.[2] microprocessor homogenizer (VirTis Co., Gardiner, NY, USA).

Determination of Encapsulation Efficiency (EE)

Each emulsion sample was centrifuged at 6000 *g* for 5 min to remove free eugenol and large oil droplets (Minispin plus, Eppendorff, Hamburg, Germany). The supernatant was diluted 100 times in deionized water and filtered through a 0.45 μm polyvinyl difluoride (PVDF) syringe membrane to obtain the permeate for HPLC. The reversed-phase HPLC analysis was performed with an Agilent Zorbax Eclipse Plus C_{18} column (5 μm; 150 mm by 4.6 mm; Agilent, Palo Alto, CA) and a 1200 series HPLC system (Agilent Technologies, Waldbronn, Germany). The sample injection volume was 10 μL, and the detector wavelength was 274 nm. A binary solvent mixture of water and methanol was used at a linear gradient from 20% to 80% methanol within 20 min for elution [16]. The flow rate was 0.5 mL/min, and the column chamber was controlled at 25 °C. A standard curve was prepared using standard solutions with eugenol dissolved at 0.010–1.0 mg/ mL in methanol to determine the amount of eugenol dispersed in unknown samples.

Because eugenol has a water-solubility of ca. 1.35 mg/mL at 21 °C [16], the amount of eugenol dissolved in water was quantified. Excessive eugenol (10.0 mg/mL) was added into water and stirred using a stir plate at RT for at least 24 h, and then the oil content in the water phase was measured using HPLC after dilution and filtration as described above. The *EE* was then calculated using the following equation:

$$EE\% = \frac{Dispersed\ eugenol - Dissolved\ eugenol}{Total\ eugenol - Dissolved\ eugenol} \times 100 \qquad (1)$$

Dimension and Stability of Eugenol Droplets at Different pHs

The hydrodynamic diameter (D_h) was measured using a Delsa™ Nano-Zeta Potential and Submicron Particle Size Analyzer (Beckman Coulter, Inc., Brea, CA). The scattering angle was fixed at 165°. The emulsions were diluted 20

times using 10 mM phosphate buffered saline (PBS) adjusted to pH 5.0–9.0 with 1.0 M HCl or NaOH. The stability of eugenol emulsions at various pHs was evaluated by measuring *D*h after storage at RT for 1, 7, and 30 days. Three replicates were tested at each pH.

Atomic Force Microscopy (AFM)

Eugenol emulsions were diluted to a NaCas concentration of ca. 10 ppm in deionized water. Eight microliter of each sample was deposited and air-dried for 4 h on freshly cleaved mica sheets before imaging using a Multimode Nanoscope VIII microscope (FESPA, Bruker Corp., Santa Barbara, CA) with a rectangular cantilever having an aluminum reflective coating on the backside. The cantilever had a quoted force constant of 2.80 N/m and was operated in the tapping mode. The topographical images were generated at a scanning speed of 1 Hz. Mean diameter of the particles was determined from the instrument software by taking averages from at least 5 images.

Zeta (ζ)-Potential Measurement

The ζ-potential of NaCas solution and eugenol emulsions was measured using a Zetasizer Nano ZS90 instrument (Malvern Instruments, Worcestershire, UK). Samples were diluted 10 times to 2.0 mg/mL NaCas in PBS and adjusted to pH 2.0– 9.0 with 1.0 M HCl or NaOH. The ζ-potential of each sample was measured at RT for three times.

Determination of Antimicrobial Activity

Bacterial Strain and Culture Preparation

Stock cultures of *L. monocytogenes* Scott A, *E. coli* O157:H7 strain ATCC 43895, and *S.* Enteritidis were obtained from the Department of Food Science at the University of Tennessee (Knoxville, TN, USA). Bacteria were stored at −20 °C in glycerol and transferred at least 2 times in tryptic soy broth (TSB) and grown at 32 °C for *L. monocytogenes* and 37 °C for *E. coli* O157:H7 and *Salmonella* with an interval of 24 h prior to use. Experiments were conducted for at least two repetitions using independent cultures, each tested in duplicate.

Minimum Inhibitory Concentration (MIC) and Minimum Bactericidal Concentration (MBC)

A free eugenol stock solution was prepared by dissolving 2.0 g eugenol in 10.0 mL 50.0% *v*/v aqueous ethanol followed by diluting for 10 times in

distilled water to 20.0 mg/mL eugenol, corresponding to 5% v/v ethanol. The stock solution was further diluted in TSB to eugenol concentrations of 0.20, 0.40, 0.60, 0.80, 1.0, 1.2, 1.5, 2.0, 2.5, and 3.0 mg/mL as working solutions. The emulsion with 38.5 mg/mL eugenol and 20.0 mg/mL NaCas was also diluted in TSB to corresponding eugenol concentrations as working samples. The bacterial culture was diluted to about 10^6 CFU/mL in TSB, and 120 µL of the diluted culture was added into wells of a 96-well microtiter plate. Each well was then added with 120 µL of TSB or an antimicrobial sample. The plates were then incubated at 32 °C for *L. monocytogenes* or 37 °C for *E. coli* O157:H7 and *Salmonella* for 24 h. The absorbance at 630 nm of each well was measured before and after 24-h incubation (ΔAbs_{630}) with a microtiter plate reader (Titertek Multiscan MC, Labsystems, Helsinki, Finland). The MIC was defined as the lowest eugenol concentration corresponding to ΔAbs_{630} smaller than 0.05. To determine MBC, 10 µL mixture from the negative wells (i.e., $\Delta Abs_{630}<0.05$) was spread on tryptic soy agar (TSA) plates and incubated for 24 h at 32 °C for *L. monocytogenes* or 37 °C for *E. coli* O157:H7 and *Salmonella*. MBC was determined as the lowest eugenol concentration corresponding to no detectable colonies after incubation.

Growth Kinetics in TSB

To study growth kinetics of bacteria in TSB, the bacterial culture was mixed with different amounts of free or encapsulated eugenol working samples prepared as in the previous section at an overall population of ca. 10^6 CFU/mL and an eugenol content corresponding to MIC or one-half of MIC. The mixtures were incubated at 32 °C for *L. monocytogenes* or 37 °C for *E. coli* O157:H7 and *Salmonella*. After incubation for 0, 4, 8, 24, and 48 h, the cultures were diluted in 0.1% peptone serially, and 0.10 mL of the diluted mixture was spread on TSA plates. The TSA plates were incubated for 24 h at 32 °C for *L. monocytogenes* or 37 °C for *E. coli* O157:H7 and *Salmonella* before counting the number of colonies.

Biophysical Properties of Bacteria after Eugenol Treatment

The emulsion prepared with an overall eugenol concentration of 38.5 mg/mL was used to study differences in the following biophysical properties of bacteria before and after treatment, in comparison to free eugenol. Free eugenol prepared at 20.0% *v*/v in 50% aqueous ethanol and the emulsion were diluted to different concentrations with TSB for scanning electron microscopy (SEM) or PBS for the other two assays. Where applicable, the positive control of an emulsion was the solution with a same amount of NaCas, while that of free eugenol was the same concentration of aqueous ethanol.

Scanning Electron Microscopy

Bacteria after treatment by 2.0 mg/mL free or encapsulated eugenol at RT for 1 h were fixed in 3% glutaraldehyde in 0.1 M sodium cacodylate buffer for 1 h at RT. After rinsing in the buffer for 3 times, samples were post-fixed in 2% osmium tetroxide. The samples after rinsing were dehydrated through a graded ethanol series from 25% to 100%. The structures of samples were imaged using a model LEO 1525 microscope (LEO Electron Microscopy, Oberkochen, Germany).

Membrane Permeability Measured with the Crystal Violet Assay

Alteration in membrane permeability after antimicrobial treatments was studied using the crystal violet assay [15]. *E. coli* O157:H7, *Salmonella*, and *L. monocytogenes* in TSB were harvested at 4300 *g* for 4 min, washed twice with 0.1 M PBS (pH 7.4), and re-suspended in PBS. An antimicrobial sample with 1.8 mg/mL eugenol or an antimicrobial control was added to the cell suspensions and incubated at 37 °C or 32 °C for 1 h. After incubation, cells were harvested at 6700 *g* for 5 min and resuspended in 2 mL PBS containing 10 μg/mL of crystal violet. After incubating for another 15 min, the suspensions were centrifuged at 13,400 *g* for 15 min and the absorbance of the cell free supernatant was measured at 590 nm (Abs_{cell}). The absorbance at 590 nm of the PBS with 10 μg/mL crystal violet (Abs_{PBS}) was also measured. The percentage of crystal violet uptake in a cell suspension was calculated using the following equation.

$$Uptake\ (\%) = \left(1 - \frac{Abs_{cell}}{Abs_{PBS}}\right) \times 100 \quad (2)$$

Estimation of Intra- and Extracellular Adenosine Triphosphate (ATP) Contents

The intracellular and extracellular ATP concentrations were measured according to a literature method [17]. The suspensions containing ~9 log CFU/mL bacteria were centrifuged at 4300 *g* for 2 min to harvest cells. After re-suspension in 0.1 M PBS (pH 7.4), 1 mL suspension with ca. ~8 log CFU/mL bacteria was treated with 30, 60 or 100 μL of a sample containing 20.0 mg/mL free or encapsulated eugenol. After incubation for 20 min at RT, the bacteria were harvested at 4300 *g*. The supernatants with extracellular matter were collected and immediately moved to an ice bath before further analysis. After decanting the supernatant, cells were resuspended in 1.0 mL of 0.5% *w/v* trichloroacetic acid buffer and then centrifuged immediately at 13,400 *g* for 10 min. The supernatant containing intracellular materials was

neutralized with 4-fold volume of 0.1 M PBS (pH 7.4) and then stored in an ice bath to prevent ATP loss.

The Enliten™ ATP Assay system with a bioluminescence detection kit (Promega, Madison, WI) was used for ATP measurement following the manual. Briefly, the rL/L reagent was rehydrated in the reconstitution buffer and incubated at RT for 1 h before use. Ten microliter of a sample and 100 μL of the reagent solution were added into wells of a 96-well microtiter plate, and the luminescence values were measured with a model Synergy HT reader (BioTek, Winooski, VT). An ATP standard curve was established using the ATP standard and ATP-free water from the kit supplier to determine the intra- and extracellular ATP concentrations. Experiments were conducted for three repetitions with independent cultures.

Statistical Analysis

All experiments were carried out at least in duplicate. All results were reported for the mean ± standard deviation (SD) of replicates. The one-way analysis of variance of treatments was performed at a significance level (*P*) of 0.05 using the least significant difference method assisted with SPSS 16.0 statistical analysis system (SPSS Inc., Chicago, IL, USA).

Results

Encapsulation Properties and Droplet Dimensions of Eugenol Emulsions

The properties of 20.0 mg/mL NaCas encapsulating eugenol at the studied conditions are shown in Table 1. The amount of eugenol dispersed in emulsions was the highest (38.0 mg/mL) when eugenol was used at an overall concentration of 74.1 mg/mL. Therefore, emulsifying eugenol with NaCas greatly improved the amount of eugenol dispersed in water. The amount of eugenol dissolved in water at RT was quantified to be 1.5 mg/mL. The *EE*% after calibration of the dissolved eugenol (eq. 1) decreased when a higher amount of eugenol was used in preparation. No noticeable phase separation was observed for emulsions prepared with an overall eugenol concentration of 38.5 mg/mL and lower (supplementary Fig. S1, following the *References*), and these emulsions had an *EE%* of 86% or higher (Table 1). Phase separation observed for emulsions with a total eugenol concentration of 74.1 mg/mL and higher corresponded to low *EE%*. Therefore, only emulsions with an overall eugenol content of 38.5 mg/mL and lower were studied further. Emulsions prepared with a higher amount of eugenol had a significantly smaller D_h (Table 2). Because homogenization itself had no significant impact

on the D_h of NaCas, encapsulation of eugenol caused the reduction of D_h. The reduced dimension of NaCas after encapsulating eugenol was also observed in AFM (Fig. 1), which showed more uniform and spherical particles after emulsification. The average particle diameter from AFM decreased from 123.2 nm of NaCas to 106.3 and 84.5 nm for emulsions prepared with 5.0 and 38.5 mg/mL eugenol, respectively. The emulsion prepared with 38.5 mg/mL eugenol was used in following studies.

Stability of Eugenol Emulsions at Different pHs

The pH stability of emulsions diluted to 1.9 mg/mL eugenol is shown in Fig. 2. The diluted emulsions were transparent at a pH of 5.0 and above, and those at alkaline pH appeared yellow. Precipitation was observed when pH was lower than 5.0. To evaluate the storage stability of emulsions at pH 5.0–9.0, D_h was measured after storage at RT for 1, 7, and 30 days (Fig. 3). There was no significant increase of droplet size in the first 7 days ($P > 0.05$), with D_h ranging from 100 to 125 nm. Except for the pH 5.0 treatment showing some precipitation, D_h increased significantly ($P < 0.05$) after 30-day storage. Nevertheless, the D_h of the emulsions at pH 5.0–9.0 before and after storage was still smaller than that of NaCas at pH 7.0 without eugenol (~150 nm, Table 2).

The ζ-potential of NaCas with and without eugenol at pH 2.0–9.0 is presented in Fig. 4. The ζ-potential of NaCas decreased from 23.7 to −35.0 mV when pH increased from 3.0 to 9.0, and a ζ-potential close to 0 mV was observed at around pH 4.5. After encapsulating eugenol, a more negative ζ-potential with a magnitude above 30 mV was observed at pH 5 and above.

MIC and MBC of Eugenol

MICs and MBCs of free (pre-dissolved in ethanol) and emulsified eugenol against Gram-positive *L. monocytogenes* and Gram-negative *E. coli* O157:H7 and *Salmonella* are presented in Table 3. The MICs of both free and encapsulated eugenol were 1.2, 0.6, and 0.6 mg/mL when tested against *L. monocytogenes, E. coli* O157:H7, and *Salmonella,* respectively. The encapsulation also did not show a significant effect on the MBCs against *L. monocytogenes* (2.0 mg/mL) or *E. coli* O157:H7 (0.8 mg/mL), while the encapsulated eugenol had a slightly lower MBC than free eugenol (0.8 vs 1.0 mg/ mL) against *Salmonella*.

Growth Kinetics of Bacteria in TSB

The antimicrobial activities of free and encapsulated eugenol were also compared for the growth kinetics shown in Fig. 5. The growth curves of controls

with and without NaCas were similar. When free and encapsulated eugenol was studied at one-half of MIC, the growth of all three bacteria was delayed but not inhibited. At an eugenol concentration equivalent to MIC, the growth kinetics was different for each bacterium. An initial reduction of *L. monocytogenes* up to 4 h was observed for both free and encapsulated eugenol treatments, followed by a significant recovery (Fig. 5a). For *E. coli* O157:H7 (Fig. 5b), free eugenol showed a reduction by ~1 log CFU/ mL after 8 h, followed by growth to the inoculation level after 24 h, which contrasted with a reduction of ca. 3 log CFU/mL in 8 h by the same concentration of encapsulated eugenol followed by insignificant changes after 24 and 48 h. Eugenol was the most effective against *Salmonella*, showing a gradual reduction to the detection limit in 24 h followed by a minor recovery after 48 h (Fig. 5c).

Changes of Bacterial Morphology after Eugenol Treatments

Figure 6 shows the SEM micrographs of bacteria after treatment by 2.0 mg/ mL free or encapsulated eugenol. *E. coli* O157:H7 and *Salmonella* cells not treated by eugenol showed an irregular and striated surface characteristic of Gram-negative bacteria, while *L. monocytogenes* exhibited a smooth surface. For the two Gram-negative bacteria, both eugenol treatments induced the damage of cell structures, showing the roughening and collapse of rod-like morphology. *L. monocytogenes* cells after free eugenol treatment either showed unnoticeable changes in the shape or surface smoothness or were completely destroyed (Fig. 6a2). Based on estimations from at least 5 SEM micrographs, about 39% and 80% *L. monocytogenes* maintained the rod-like morphology after treatment by free and encapsulated eugenol, respectively.

Intra- and Extracellular ATP Concentrations

The intra- and extracellular ATP concentrations of the three bacteria after being treated with free and encapsulated eugenol were measured to better understand the potential antibacterial mechanism (Fig. 7). Controls without antimicrobial treatments showed intra- and extracellular ATP levels of 0.036 and 0.0039 nmol for *L. monocytogenes*, 0.045 and 0.0048 nmol for *E. coli* O157:H7, and 0.031 and 0.0024 nmol for *Salmonella*, respectively. NaCas alone did not show any significant effect on either intra- or extracellular ATP concentrations of all three bacteria (data not shown).

When treated by free eugenol up to 2.0 mg/mL, no significant difference in the extracellular ATP of any of the three bacteria was observed ($P > 0.05$). No decrease in the intracellular ATP concentration was observed at 0.6–2.0 mg/mL of free eugenol for *L. monocytogenes,* 0.6 mg/mL for *E. coli* O157:H7, and 0.6–1.2 mg/mL for *Salmonella*. In contrast, a significant reduction of intracellular ATP concentration was observed for *E. coli* O157:H7 and

Salmonella treated by 0.6 mg/mL and more encapsulated eugenol, as well as *L. monocytogenes* treated with 1.2 and 2.0 mg/ml encapsulated eugenol ($P < 0.05$). A significant reduction of intracellular ATP of bacteria treated with a sufficiently high amount of encapsulated eugenol corresponded to a significant increase in extracellular ATP.

The Uptake of Crystal Violet by Bacteria after Eugenol Treatments

Figure 8 shows the uptake of crystal violet after treatments with and without 1.8 mg/mL free or encapsulated eugenol. NaCas showed no obvious effect on the uptake of crystal violet by the bacteria. All bacteria showed an increased uptake of crystal violet after treatment with free or encapsulated eugenol. The crystal violet uptake by *L. monocytogenes* after free eugenol treatment was higher than the control, while the increase in crystal violet uptake of the encapsulated eugenol treatment was not significant. The crystal violet uptake by *E. coli* O157:H7 after treatment with encapsulated eugenol was not significantly different from that of free eugenol treatment ($P > 0.05$). Lastly, the crystal violet uptake by *Salmonella* after treatment by encapsulated eugenol was significantly higher than the free eugenol treatment ($P < 0.05$).

Discussion

Physical Properties of Eugenol Nanoemulsions

Emulsions with droplets smaller than 125 nm (Table 2; Fig. 1) and overall good kinetic stability (Fig. 3) were prepared with 20.0 mg/mL NaCas and up to 38.5 mg/mL eugenol (Table 1), and the EE% was higher than 86% (Table 1). These characteristics were better than 50 mg/mL NaCas emulsifying up to 10 mg/mL thymol as stable dispersions [14]. NaCas consists of mixtures of α_{s1}-, α_{s2}-, β-, and κ-caseins at proportions of approximately 4:1:4:1 that are all known to be surface active, with β-casein being recognized for the greatest contributor of emulsifying properties [18]. Thymol has a melting point of about 50 °C [19] and a water solubility of 0.48 mg/mL at 21 °C [16], whereas eugenol is a liquid and has a water-solubility of 1.50 mg/mL at 21 °C measured in the present study, with the latter agreeing with the previously reported solubility of 1.35 mg/mL [16]. The higher hydrophilicity of eugenol than thymol results in a lower oil/water interfacial tension and the higher fluidity (liquid vs. solid) lowers the viscosity of the dispersed phase during emulsification, which favor emulsion formation during shear homogenization. Additionally, NaCas is hydrophilic and is expected to have a hydrophile-lipophile balance closer to eugenol than thymol. These factors can

contribute to the better capacity of NaCas emulsifying eugenol in the present study than that of thymol [14].

A smaller dimension of emulsions with a higher content of eugenol was observed both in dynamic light scattering (Table 2) and AFM (Fig. 1). The observation is in contrast with the expectation of larger droplets at a higher oil concentration because of the reduced surfactant-to-oil ratio during homogenization [20], as shown for oregano EO emulsified into an aqueous phase containing chitosan-tripolyphosphate nanoparticles and Tween 80 [21]. NaCas is composed of structures with a dimension of 10–20 nm and some indicate loosely associated proteins when observed in transmission electron microscopy [22]. Caseins are also known to be intrinsically disordered proteins with little higher order structures [23]. These characteristics of NaCas can contribute to a dimension of >100 nm measured in DLS (Table 2) and AFM, after drying on a mica sheet (Fig. 1). As previously discussed [14], emulsification of eugenol and hydrophobic attraction by eugenol improve the compactness of particulate structures containing NaCas, which reduces the dimension measured in DLS and AFM.

Caseins have an isoelectric point at pH 4.6 [10], and dispersions with poor stability below pH 5.0 (Fig. 2) are characteristics of caseins. The yellow color of emulsions at alkaline pH can be attributed to the increased water solubility of eugenol due to deprotonation of hydroxyl groups [10, 22]. Above pH 5.0, emulsions have a zeta-potential magnitude of >30 mV which can typically provide repulsive electrostatic interactions strong enough to stabilize colloidal particles against aggregation [24, 25]. NaCas is also known to provide steric stabilization when present at the surface of colloidal particles [25]. Therefore, eugenol emulsions had insignificant changes in D_h at pH 5.0–9.0 within 7 days at RT (Fig. 3). As discussed previously, eugenol is slightly soluble in water, and the solubility is higher at a higher pH. This can cause Ostwald ripening that results from the higher solubility of eugenol in smaller droplets, which causes the dissolving out of eugenol to join bigger droplets with a lower Laplace pressure [25]. The growth of droplets, more apparent at a higher pH, was therefore evident after storage for 30 days (Fig. 3). Changes in emulsion droplet size after 30-day storage may have accounted for some precipitation at pH 5.0, since eugenol is slightly denser than water at RT [19].

Antimicrobial Properties of Eugenol Nanoemulsion

The MICs of free eugenol (Table 3) against *L. monocytogenes* (1.2 mg/mL), *E. coli* O157:H7 (0.6 mg/mL), and *Salmonella* (0.6 mg/mL) agreed with a previous study [1]. The MICs of both free and encapsulated eugenol at 32 or 37 °C are similar (Table 3) and are all lower than the water solubility of 1.5 mg/mL at 21 °C. The encapsulated eugenol partitions between droplets, the

continuous aqueous phase, and bacteria due to concentration gradients. This indicates no negative impact of NaCas, which can bind with eugenol, on antimicrobial activity of eugenol. Similar explanation can be made for MBCs of free and encapsulated eugenol. When tested for growth kinetics at eugenol levels corresponding to the MICs, Gram-negative *E. coli* O157:H7 and *Salmonella* were inhibited to a greater extent by eugenol than Gram-positive *L. monocytogenes* (Fig. 5), and significant differences between free eugenol and emulsion treatments were only observed for *E. coli* O157:H7 at 37 °C. The former observation agrees with the lower MIC of Gram-negative than Gram-positive bacteria (Table 3). The latter observation can result from different membrane structures between *E. coli* O157:H7 and *Salmonella*, since disrupting bacterial membranes is a major mechanism of the antibacterial activity of eugenol [26], further discussed below.

Biophysical Properties of Bacteria Treated by Free and Nanoemulsified Eugenol

Eugenol is a multi-target antimicrobial agent, with the primary mechanism being the disruption of cell membrane through non-specific binding with lipophilic constituents of the membrane [27, 28] and the secondary mechanism being inhibitions of enzymes involved in the biosynthetic pathway [29]. The latter was studied for the inhibition of 1-deoxy-D-xylulose 5-phosphate reductoisomerase (DXR) [30], a key enzyme of the methylerythritol phosphate pathway [29]. Eugenol had a much higher activity than carvacrol, thymol, and linalool inhibiting DXR and the mode of inhibition was observed to be competitive, indicating the specificity of binding between eugenol and DXR [29, 30]. These mechanisms may be used to understand impact of nanoencapsulation on eugenol-bacterium interactions based on the measured biophysical properties, although variations in eugenol concentration, bacterial population, and treatment temperature and duration adopted for different assays may not allow direct correlation of all sets of data.

Compared to Gram-negative bacteria with an envelope consisting of an outer membrane containing lipopolysaccharides, a peptidoglycan cell wall, and an inner cytoplasmic membrane, Gram-positive bacteria lack of the outer membrane, making it easier to change structures after interacting with antimicrobials [31, 32]. The structural differences of Gram-negative and Gram-positive bacteria agree with a significant portion of collapsed *L. monocytogenes* cells while only morphological changes of *E. coli* O157:H7 and *Salmonella* after treatment by same amounts of eugenol (Fig. 6). When compared with free eugenol, eugenol in the emulsion partitions with NaCas and bacteria, which reduces the availability of eugenol to interact with bacteria within a limited duration. This physical phenomenon agrees with a smaller percentage of *L. monocytogenes* cell collapse after 1-h treatment by

the emulsion with 2 mg/mL eugenol than the same amount of free eugenol (39% vs. 80% based on SEM, Fig. 6). Whereas, no complete cell collapse was observed for *E. coli* O157:H7 and *Salmonella* treated by 2.0 mg/mL eugenol (Fig. 6), a level more than twice of their MBCs (Table 3). Therefore, cell death is not completely dependent on cell destruction.

Changes in bacterial morphology in Fig. 6 however are not in agreement with the crystal violet uptake% by bacteria treated with 1.8 mg/mL encapsulated or free eugenol at 32 or 37 °C for 1 h (Fig. 8). The encapsulated eugenol had similar crystal violet uptake% as free eugenol and the control treatments without antimicrobials for *L. monocytogenes* and *E. coli* O157:H7 at the studied conditions (Fig. 8). In contrast, a significant increase of crystal uptake% was observed for *Salmonella* treated by 1.8 mg/mL encapsulated eugenol than free eugenol, both of which were higher than the controls (Fig. 8). These observations are different from the lower crystal violet uptake% of the three bacteria treated by 0.2–0.9 mg/mL thyme oil nanoencapsulated by NaCas and lecithin than free thyme oil [33]. Crystal violet stains bacterial peptidoglycan, and an increased uptake of crystal violet can be correlated to an increase of non-specific permeability of cytoplasmic membrane [15]. At the assay conditions, peptidoglycan in cell debris of *L. monocytogenes* can also be available to staining by crystal violet, making the difference between encapsulated and free eugenol treatments insignificant. For the two Gram-negative bacteria, data in Fig. 8 indicate the increased permeability of cytoplasmic membrane after treating *Salmonella* with encapsulated eugenol than free eugenol, but the same is not true for *E. coli* O157:H7. This is opposite with the growth curves in Fig. 5 showing the enhanced inhibition of *E. coli* O157:H7 after encapsulation of eugenol but insignificant difference in inhibiting *Salmonella* by free and encapsulated eugenol at the MIC. Therefore, crystal violet assay results did not provide a complete interpretation of antimicrobial activities.

The trend is consistent for the ATP data in Fig. 7 after treating bacteria for a short duration of 20 min at RT. The significant reduction of intracellular ATP was observed at a lower concentration of encapsulated eugenol than free eugenol for all three bacteria. The increase of extracellular ATP of the three bacteria was significant for the emulsion treatment at a range of 0–2.0 mg/mL eugenol, while for free eugenol treatments, the increase was significant only for *E. coli* O157:H7. A depletion of intracellular ATP may be attributed to the release or loss of ATP from cells, hydrolysis in cells, and/or inhibition of membrane transport [34]. An increase of extracellular ATP concentration is due to the loss of intracellular ATP, which can be attributed to an increased degree of cytoplasmic membrane disruption [17]. The data in Fig. 7 suggest the increased permeability of emulsified eugenol than free eugenol after short-time interaction. An increase in the extracellular ATP content of both Gram-negative *Salmonella* Enteritidis and Gram-positive *Bacillus*

cereus treated by linolenic acid was also reported after addition of a surfactant, glycerol laurate or glycerol myristate, which was correlated to the enhanced antimicrobial activity of the combination [35]. Surfactants with appropriate physicochemical properties can accumulate in the membrane lipid bilayer to cause the redistribution of membrane protein and lipids, which influences the membrane function [35–37]. The adsorption of surfactants on bacterial membrane can facilitate the accumulation of antimicrobials on cell surface and the subsequent penetration into cells, which can be correlated to the observed enhancement of antimicrobial activities [35]. In addition, ionic residues of peripheral proteins can enable the binding with a membrane surface by electrostatic interactions, while aliphatic and aromatic residues of these proteins can result in the subsequent membrane penetration [38]. Therefore, the known membrane binding activities of caseins [39, 40] may have resulted in the increased extracellular ATP and decreased intracellular ATP of bacteria treated by a sufficiently high content of emulsified eugenol (Fig. 7). The observation of higher extracellular ATP content of *Salmonella* treated by encapsulated eugenol than free eugenol (Fig. 7) was in accordance with the relatively higher crystal violet uptake (Fig. 8). However, the same correlation of ATP data in Fig. 7 and crystal violet uptake data in Fig. 8 was not observed for *E. coli* O157:H7.

The data in the present study may be interpreted by also considering other known knowledge in the literature. When subjected to a stress such as antimicrobials, it is well-known that bacteria can change the composition and biophysical properties of membranes so as to adapt to survive through a stress [41, 42]. Initially, NaCas facilitates the accumulation of eugenol at the membrane and permeation into bacteria (Fig. 7) [43]. However, when given time, the adaptation of membrane can be different for each bacterium. *L. monocytogenes*, although having a significant portion of cell disruption by 2.0 mg/mL eugenol (Fig. 6), can adapt and recover to result in no significant difference in growth curves for free and encapsulated eugenol treatments at MICs (Fig. 5). For the two Gram-negative bacteria, *E. coli* O157:H7 may not be as effective as *Salmonella* adapting to the antimicrobial stress, resulting in a greater reduction by encapsulated eugenol than free eugenol at a level of MIC in the growth kinetics assay (Fig. 5). This speculation however requires future work, for example using small angel neutron scattering to study biophysical structures of model membranes after interacting with free and encapsulated eugenol [44].

Conclusions

In summary, up to 38.5 mg/mL eugenol was emulsified by 20.0 mg/mL NaCas using shear homogenization. Encapsulation of eugenol decreased the

dimension of NaCas and increased the magnitude of negative zeta potential above pH 5.0 that corresponded to stable emulsion droplet dimensions during storage up to 7 days at 21 °C. The encapsulated eugenol showed similar MICs and MBCs against *L. monocytogenes*, *E. coli* O157:H7 and *Salmonella* as eugenol pre-dissolved in ethanol. The encapsulated eugenol applied at MICs was more effective against the growth of *E. coli* O157:H7 than free eugenol at 37 °C in 48 h, but differences were insignificant for *L. monocytogenes* and *Salmonella* at 32 and 37 °C, respectively. After interaction at 21 °C for 20 min, all three bacteria showed the increased accumulation and permeation of encapsulated eugenol than free eugenol based on changes in intra- and extracellular ATP contents. However, the same trend was not observed based on examination of morphology and uptake of crystal violet. The current study points to the future direction on examining changes of membrane composition and biophysical properties to better understand mechanisms of nanoencapsulated eugenol interacting with bacteria and the correlation to antibacterial activities. The study nevertheless showed the excellent properties of NaCas emulsifying eugenol to prepare stable emulsions as intervention systems.

Tables 1–3, Figures 1–8, & Supplementary Figure S1,
Acknowledgments, and References follow.

Table 1. Properties of 20.0 mg/mL NaCas emulsifying eugenol

Overall eugenol content (mg/mL)	Dispersed eugenol (mg/mL)	Encapsulation efficiency (%)
5.0	5.0 ± 0.3^{e}	98.9 ± 6.8
9.9	9.4 ± 0.1^{d}	93.4 ± 0.6
19.6	17.2 ± 0.1^{c}	86.7 ± 0.7
38.5	33.4 ± 0.5^{b}	86.2 ± 1.1
74.1	38.0 ± 1.1^{a}	50.3 ± 1.5
137.9	36.3 ± 0.4^{a}	25.5 ± 0.3

Numbers are mean ± standard deviation from triplicate samples. Different superscript letters indicate differences in the mean of the same parameter ($P < 0.05$).

Table 2. Hydrodynamic diameter (D_h) of dispersions with various amounts of eugenol emulsified by 20.0 mg/mL NaCas at pH 7.0

Overall eugenol content (mg/mL)	D_h (nm)
0	153.8 ± 3.1 a
0#	146.3 ± 3.0 a
5.0	124.6 ± 2.7 b
9.9	117.4 ± 0.9 b
19.6	110.3 ± 1.9 bc
38.5	104.7 ± 2.0 c

Numbers are mean ± standard deviation from triplicate samples. Different superscript letters indicate differences in the mean ($P < 0.05$).

The sample was also homogenized at eugenol emulsion preparation conditions.

Table 3. Minimum inhibitory concentration (MIC) and minimum bactericidal concentration (MBC) of free (pre-dissolved in ethanol) or encapsulated eugenol against three bacteria

Bacteria	MIC (mg/mL)		MBC (mg/mL)	
	Free	Encapsulated	Free	Encapsulated
L. monocytogenes Scott A	1.2	1.2	2.0	2.0
E. coli O157:H7 ATCC 43895	0.6	0.6	0.8	0.8
Salmonella Enteritidis	0.6	0.6	1.0	0.8

NaCas showed no inhibition.

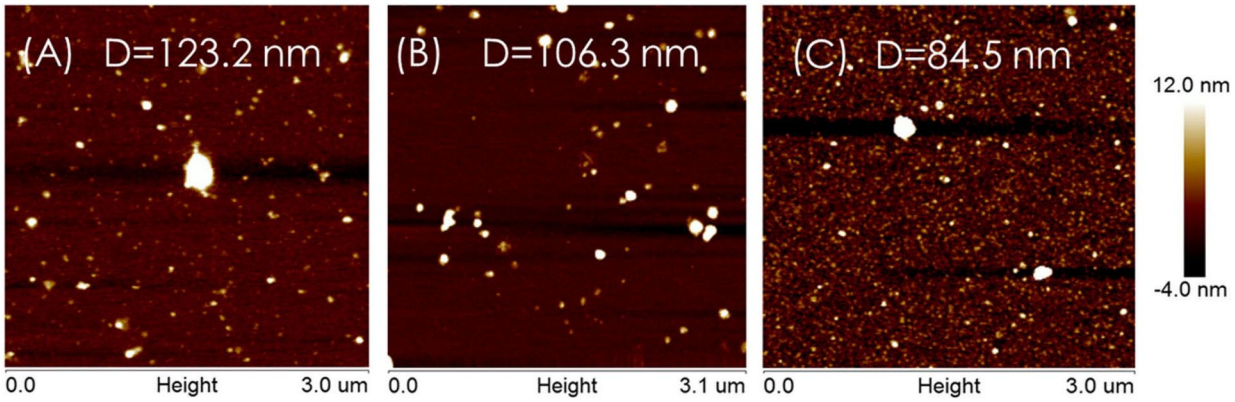

Fig. 1. AFM topography images of NaCas (a) and dispersions with 5mg/mL (b) or 38.5mg/mL (C) eugenol emulsified by 20.0 mg/mL NaCas at pH 7.0. Dispersions were diluted to ca. 0.01 mg/mL NaCas before drying for AFM. The scale on the right shows particle height

Fig. 2. Appearance of the emulsion containing 38.5 mg/mL eugenol after 20-fold dilution in PBS adjusted to pH 2.5, 3.0, 4.0, 5.0, 6.0, 7.0, 8.0 and 9.0 (from left to right)

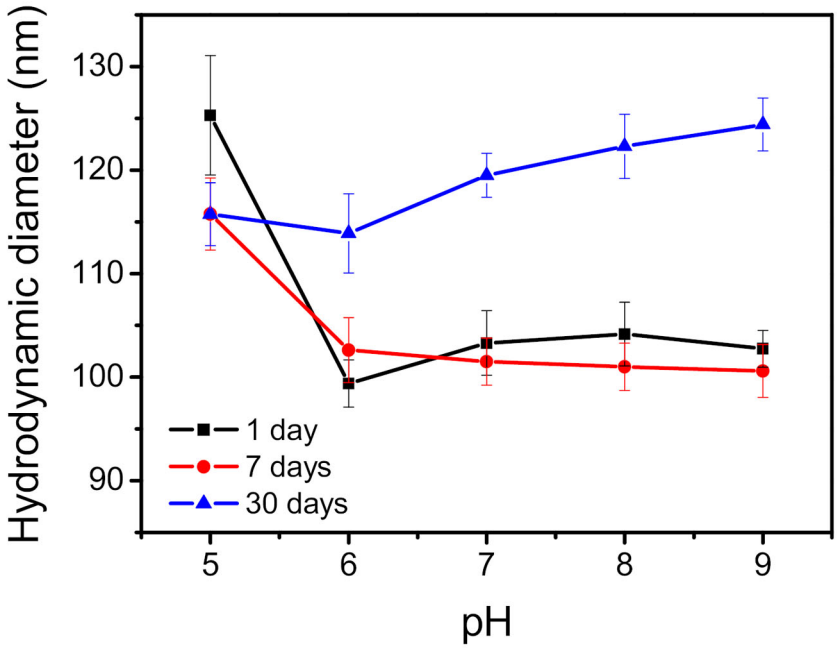

Fig. 3. Average hydrodynamic diameters of nanoemulsions with 1.9 mg/ mL eugenol after adjusting pH to 5.0–9.0 and storing at 21 °C for 1, 7, and 30 days. The emulsion was prepared with 38.5 mg/mL eugenol and diluted with PBS. Error bars are standard deviations (n = 3)

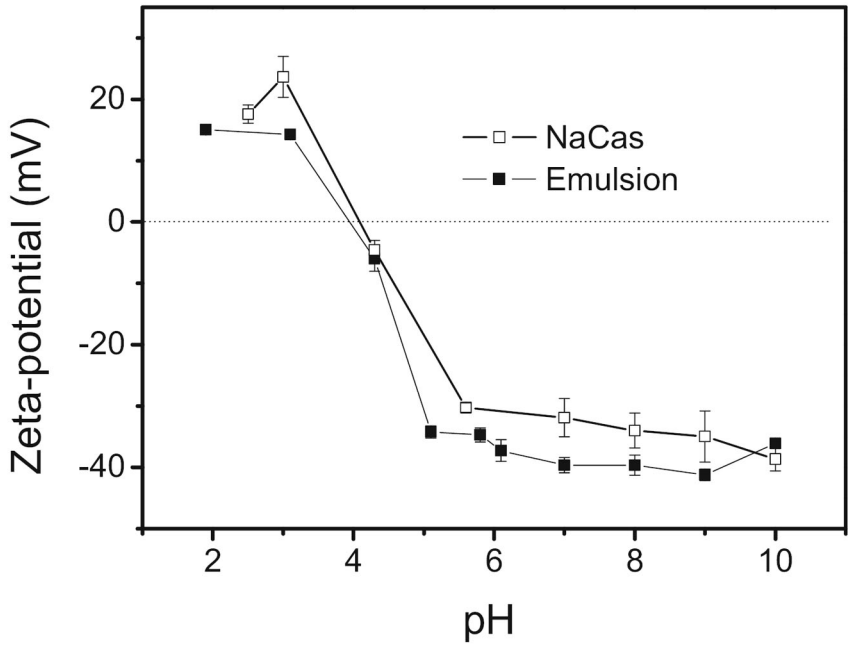

Fig. 4. Zeta-potential of 10-fold diluted dispersions with 20.0 mg/mL NaCas and the emulsion prepared with 38.5 mg/mL eugenol and 20.0 mg/mL NaCas. The samples were adjusted to pH 2.0–9.0 and diluted 10 times in PBS adjusted to the same pH before measurements. Error bars are standard deviations (n = 3)

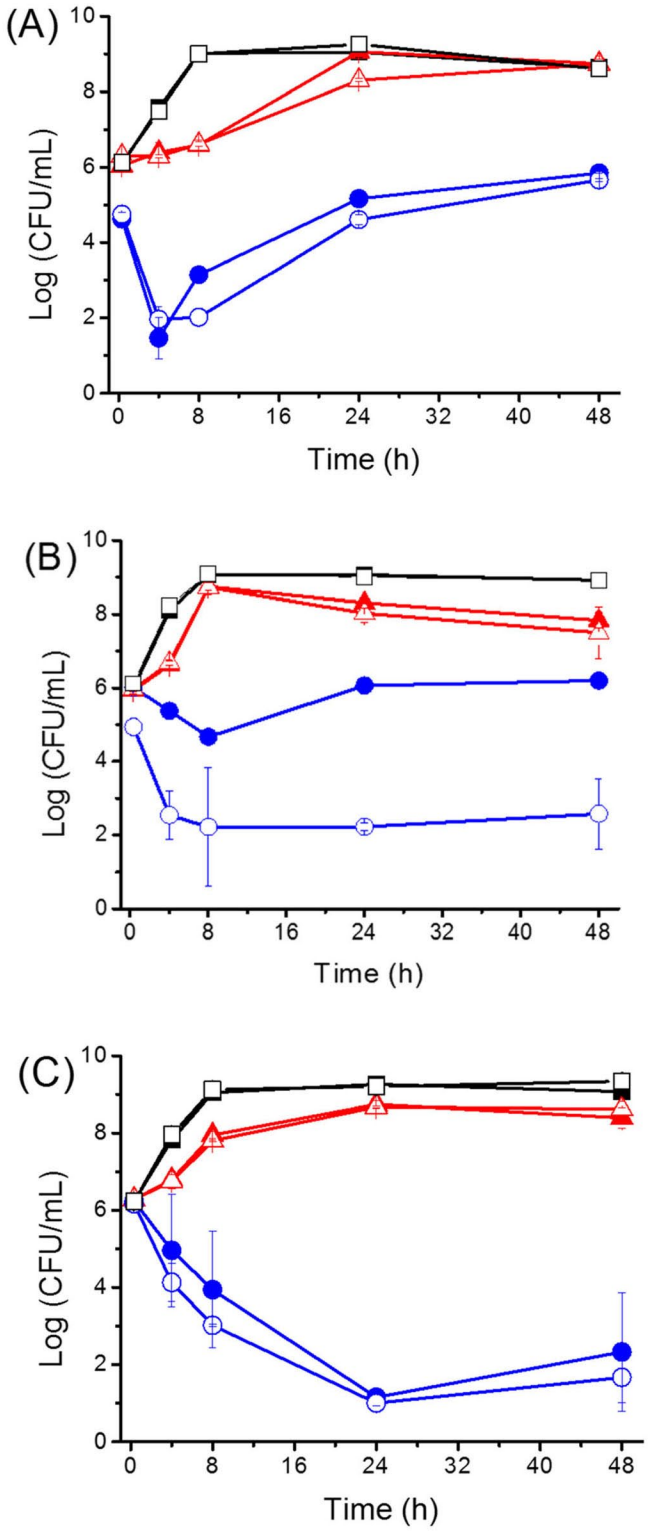

Fig. 5. The growth curves of *L. monocytogenes* at 32 °C **(a)**, *E. coli* O157:H7 at 37 °C **(b)** and *Salmonella* at 37 °C **(c)** in TSB treated by nothing (negative control, black filled square), 0.6 mg/mL NaCas (black open square), free eugenol (pre-dissolved in 5% ethanol) at MIC (blue filled circle) and one-half of MIC (red filled triangle), or encapsulated eugenol at MIC (blue open circle) and one-half of MIC (red open triangle). Detection limit is 1.0 log CFU/mL. Error bars are standard deviations (n = 3)

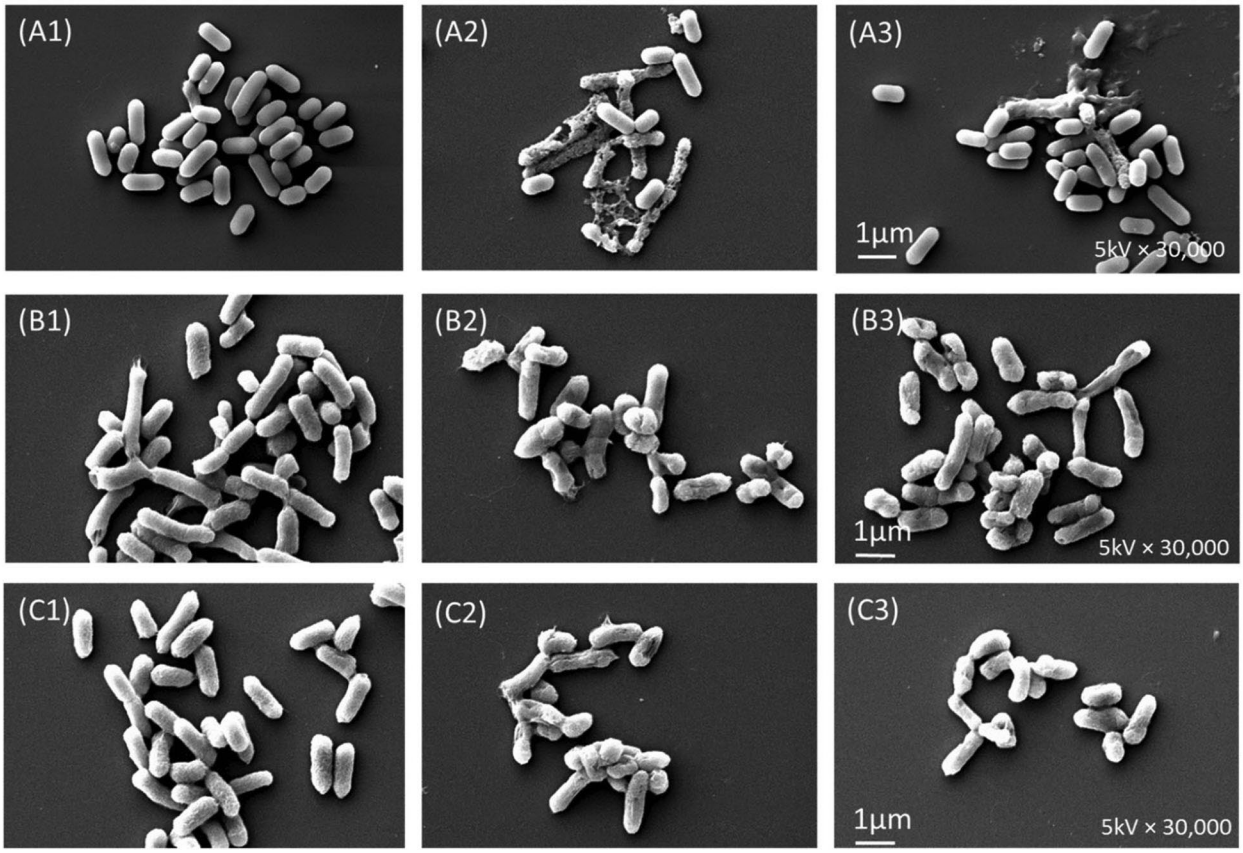

Fig. 6. SEM micrographs of *L. monocytogenes* **(a)**, *E. coli O157:H7* **(b)** and *Salmonella* **(c)** received no treatment **(1)** or after treatment with 2.0 mg/mL free eugenol pre-dissolved in ethanol **(2)** or 2.0 mg/mL eugenol encapsulated by NaCas **(3)** for 1 h at 21 °C

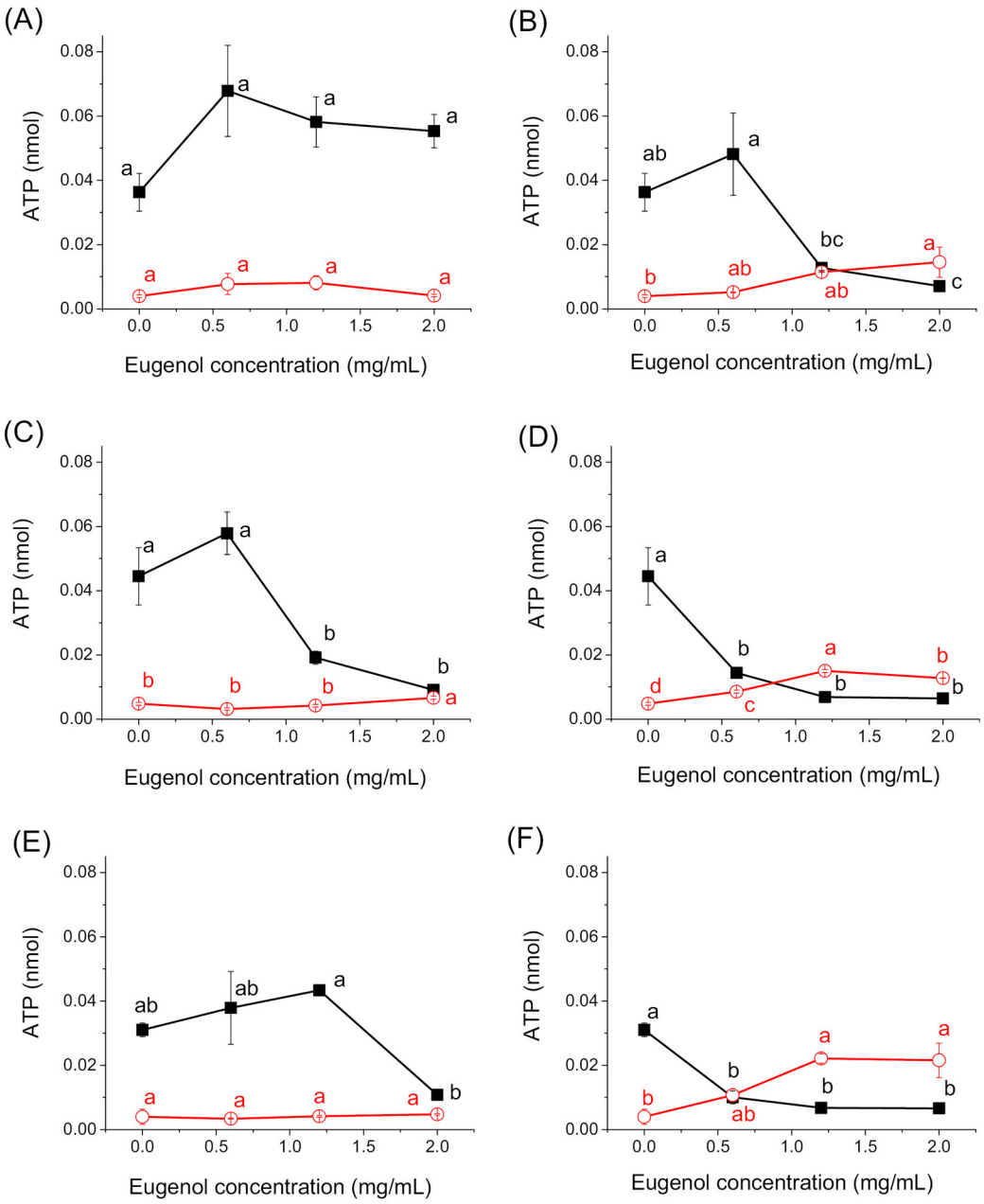

Fig. 7. Intra- (black square) and extracellular (red circle) ATP concentrations of *L. monocytogenes* **(a, b)**, *E. coli* O157:H7 (c, d), and *Salmonella* **(e, f)** treated by different amounts of free **(a, c, e)** or encapsulated **(b, d, f)** eugenol at 21 °C for 20 min. Error bars are standard deviations (n = 3). Different letters indicate significant differences of treatments on the same curve

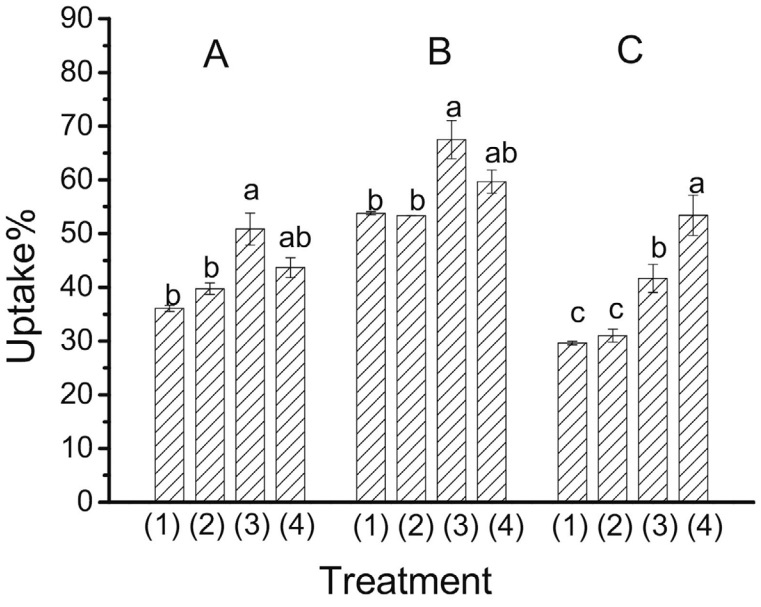

Fig. 8. The uptake% of crystal violet by *L. monocytogenes* at 32 °C **(a)**, *E. coli* O157:H7 at 37 °C **(b)**, and *Salmonella* at 37 °C **(c)** after 1-h treatment by: **(1)** no additional compound; **(2)** 1.8 mg/mL NaCas; **(3)** 1.8 mg/mL eugenol pre-dissolved in 5% ethanol, and **(4)** 1.8 mg/mL encapsulated eugenol with 2.0 mg/mL NaCas. Error bars are standard deviations (n = 3). Different letters above bars indicate significant differences in the mean of the same bacterium treatments

Acknowledgments — The authors sincerely thank Dr. Yangchao Luo for assisting SEM experiments. This work was supported by The University of Tennessee, the USDA NIFA Hatch Project 223984 and TEN02010-03476, and Dairy Research Institute (Rosemont, IL, USA). Any opinions, findings, conclusions, or recommendations expressed in this publication are those of the authors and do not necessarily reflect the view of the U.S. Department of Agriculture.

References

1. S. Burt, Int. J. Food Microbiol. 94, 223 (2004). doi 10.1016/j.ijfoodmicro.2004.03.022
2. K. Ziani, Y. Chang, L. McLandsborough, D.J. McClements, J. Agric. Food Chem. 59, 6247 (2011). doi 10.1021/jf200450m
3. C. Beristain, H. Garcıa, E. Vernon-Carter, LWT-Food Sci. Technol. 34, 398 (2001)
4. D.A. Rodea-González, J. Cruz-Olivares, A. Román-Guerrero, M.E. Rodríguez-Huezo, E.J. Vernon-Carter, C. Pérez-Alonso, J. Food Eng. 111, 102 (2012). doi 10.1016/j.jfoodeng.2012.01.020

5. C. Liolios, O. Gortzi, S. Lalas, J. Tsaknis, I. Chinou, Food Chem. 112, 77 (2009). doi 10.1016/j.foodchem.2008.05.060
6. M.-J. Choi, A. Soottitantawat, O. Nuchuchua, S.-G. Min, U. Ruktanonchai, Food Res. Int. 42, 148 (2009). doi 10.1016/j.foodres.2008.09.011
7. S. Gaysinsky, T.M. Taylor, P.M. Davidson, B.D. Bruce, J. Weiss, J. Food Prot. 70, 2631 (2007). doi 10.4315/0362-028X-70.11.2631
8. Q. Ma, P.M. Davidson, Q. Zhong, Int. J. Food Microbiol. 166, 77 (2013). doi 10.1016/j.ijfoodmicro.2013.06.017
9. E.N. Frankel, S.-W. Huang, R. Aeschbach, E. Prior, J. Agric. Food Chem. 44, 131 (1996). doi 10.1021/jf950374p
10. Y. Zhang, Q.X. Zhong, Food Hydrocoll 33, 1 (2013). doi 10.1016/j.foodhyd.2013.02.009
11. K. Pan, Q. Zhong, S.J. Baek, J. Agric. Food Chem. 61, 6036 (2013). doi 10.1021/jf400752a
12. H.Q. Chen, Y. Zhang, Q.X. Zhong, J. Food Eng. 144, 93 (2015). doi 10.1016/j.jfoodeng.2014.07.021
13. J. Xue, Q. Zhong, J. Agric. Food Chem. 62, 9900 (2014). doi 10.1021/jf5034366
14. K. Pan, H. Chen, P.M. Davidson, Q. Zhong, J. Agric. Food Chem. 62, 1649 (2014). doi 10.1021/jf4055402
15. K.P. Devi, S.A. Nisha, R. Sakthivel, S.K. Pandian, J. Ethnopharmacol. 130, 107 (2010). doi 10.1016/j.jep.2010.04.025
16. H. Chen, P.M. Davidson, Q. Zhong, App. Environ. Microbiol. 80, 907 (2014). doi 10.1128/AEM.03010-13
17. M. Oussalah, S. Caillet, M. Lacroix, J. Food Prot. 69, 1046 (2006). doi 10.4315/0362-028X-69.5.1046
18. M. Srinivasan, H. Singh, P.A. Munro, J. Agric. Food Chem. 44, 3807 (1996). doi 10.1021/jf960135h
19. NIST. NIST WEBbook; http://webbook.nist.gov/chemistry (accessed Dec. 6, 2017)
20. N. Terjung, M. Loffler, M. Gibis, J. Hinrichs, J.Weiss, Food Funct. 3, 290 (2012). doi 10.1039/C2FO10198J
21. S.F. Hosseini, M. Zandi, M. Rezaei, F. Farahmandghavi, Carbohydr. Polym. 95, 50 (2013). doi 10.1016/j.carbpol.2013.02.031
22. K. Pan, Y. Luo, Y. Gan, S.J. Baek, Q. Zhong, Soft Matter 10, 6820 (2014). doi 10.1039/C4SM00239C
23. R. van der Lee et al., Chem. Rev. 114, 6589 (2014)
24. H. Bouzid, M. Rabiller-Baudry, L. Paugam, F. Rousseau, Z. Derriche, N.E. Bettahar, J. Membrane Sci. 314, 67 (2008). doi 10.1016/j.memsci.2008.01.028
25. E. Dickinson, Food Hydrocoll 23, 1473 (2009). doi 10.1016/j.foodhyd.2008.08.005
26. S. Hemaiswarya, M. Doble, Phytomedicine 16, 997 (2009). doi 10.1016/j.phymed.2009.04.006
27. K. Knobloch, A. Pauli, B. Iberl, H. Weigand, N. Weis, J. Essent. Oil Res. 1, 119 (1989). doi 10.1080/10412905.1989.9697767

28. A. Gill, R. Holley, Int. J. Food Microbiol. 108, 1 (2006). doi 10.1016/j.ijfoodmicro.2005.10.009
29. M. Rohmer, in *Comprehensive natural products II: Chemistry and Biology*, edited by L. Mander, and H.-W. Liu (Newnes, 2010), pp. 517
30. X. Hui, G. Yan, F.-L. Tian, H. Li, W.-Y. Gao, Med. Chem. Res. 26, 442 (2016)
31. H.A. Bladen, S.E. Mergenhagen, J. Bacteriol. 88, 1482 (1964)
32. M. Kong, X.G. Chen, K. Xing, H.J. Park, Int. J. Food Microbiol. 144, 51 (2010). doi 10.1016/j.ijfoodmicro.2010.09.012
33. J. Xue, P.M. Davidson, Q. Zhong, Int. J. Food Microbiol. 210, 1 (2015). doi 10.1016/j.ijfoodmicro.2015.06.003
34. T. Ohta, K. Nagano, M. Yoshida, P. Natl, Acad. Sci. USA 83, 2071 (1986). doi 10.1073/pnas.83.7.2071
35. J.-Y. Lee, Y.-S. Kim, D.-H. Shin, J. Agric. Food Chem. 50, 2193 (2002). doi 10.1021/jf011175a
36. J. Sikkema, J. De Bont, B. Poolman, Microbiol. Rev. 59, 201 (1995)
37. P.D. Cani, A. Everard, Trend. Endocrinol. Met. 26, 273 (2015). doi 10.1016/j.tem.2015.03.009
38. R.V. Stahelin, W. Cho, Biochemistry 40, 4672 (2001). doi 10.1021/bi0020325
39. M. Sokolovski, T. Sheynis, S. Kolusheva, R. Jelinek, BBA Biomembranes 1778, 2341 (2008). doi 10.1016/j.bbamem.2008.07.001
40. T. Hira, H. Hara, F. Tomita, Y. Aoyama, Exp. Biol. Med. 228, 850 (2003). doi 10.1177/15353702-0322807-11
41. F. Nazzaro, F. Fratianni, L. De Martino, R. Coppola, V. De Feo, Pharmaceuticals (Basel) 6, 1451 (2013). doi 10.3390/ph6121451
42. Y.M. Zhang, C.O. Rock, Nat. Rev. Microbiol. 6, 222 (2008). doi 10.1038/nrmicro1839
43. R.Y. Chiou, R.D. Phillips, P. Zhao, M.P. Doyle, L.R. Beuchat, Appl. Environ. Microbiol. 70, 2204 (2004). doi 10.1128/AEM.70.4.2204-2210.2004
44. F. Foglia, A.F. Drake, A.E. Terry, S.E. Rogers, M.J. Lawrence, D.J. Barlow, BBA-Biomembranes 1808, 1574 (2011). doi 10.1016/j.bbamem.2011.02.012